frontiers | Frontiers in Environmental Science

TYPE Data Report
PUBLISHED 17 January 2023
DOI 10.3389/fenvs.2023.976113

OPEN ACCESS

EDITED BY
Jian Liu,
Division of Environment and Natural Resources, Norwegian Institute of Bioeconomy Research (NIBIO), Norway

REVIEWED BY
Thang Phan,
Vietnam Academy of Science and Technology, Vietnam
Soo-Jin Park,
Inha University, Republic of Korea

*CORRESPONDENCE
Zhiliang Yao,
yaozhl@th.btbu.edu.cn
Jian Yu,
yujian@ipe.ac.cn

SPECIALTY SECTION
This article was submitted to Atmosphere and Climate, a section of the journal Frontiers in Environmental Science

RECEIVED 23 June 2022
ACCEPTED 02 January 2023
PUBLISHED 17 January 2023

CITATION
Li C, Zhao S, Li M, Yao Z, Li Y, Zhu C, Xu S-M, Li J and Yu J (2023), The effect of the active carbonyl groups and residual acid on the ammonia adsorption over the acid-modified activated carbon. *Front. Environ. Sci.* 11:976113. doi: 10.3389/fenvs.2023.976113

The effect of the active carbonyl groups and residual acid on the ammonia adsorption over the acid-modified activated carbon

Changming Li[1], Shuying Zhao[1,2], Ming Li[1], Zhiliang Yao[1]*, Yang Li[2], Chuanqiang Zhu[3], Si-Min Xu[4], Junjie Li[5] and Jian Yu[2]*

[1]State Environmental Protection Key Laboratory of Food Chain Pollution Control, School of Ecology and Environment, Beijing Technology and Business University, Beijing, China, [2]State Key Laboratory of Multi-phase Complex System, Institute of Process Engineering, Chinese Academy of Sciences, Beijing, China, [3]Everbright Environmental Technology (China) Co., Ltd., Incineration Technology Research Institute, Nanjing, China, [4]College of Chemistry, Beijing University of Chemical Technology, Beijing, China, [5]National Engineering Research Center of Sintering and Pelletizing Equipment System, Zhongye Changtian International Engineering Co., Ltd., Changsha, China

KEYWORDS

NH_3 removal, activated carbon, acid modification, co-adsorption mechanism, hydrogen-bond network

1 Introduction

Ammonia (NH_3) is a highly toxic and extremely corrosive pollutant, which may bring undesired odors, lead to severe burning of respiratory systems, and contribute to fine particulate matter (PM2.5) concentration in the atmospheric environment (Stokstad 2014; Han et al., 2021; Jiang et al., 2022). Many different sources can release NH_3, including home/public toilets, farm manure, liquid NH_3 refrigerants, construction waste antifreeze, expansion agents, industrial desulfurization/denitrification units (Dai et al., 2019; Zhong et al., 2019; Liang et al., 2020). In recent years, ammonia pollution has caused increasing concerns about the environment and human health around the world, and rigid standards (e.g., National Emission Ceilings Directive 2016/2284/EU, GB/T 34340-2017) have been put out to restrict the ammonia emission (Wang et al., 2017a; Giannakis et al., 2019). Generally, NH_3 removal technologies include catalytic oxidation, biological processes, membrane technology, and scrubbing processes (Vikrant et al., 2017). Although the high removal efficiency of NH_3 can be achieved, they may still suffer possible problems such as temperature/pressure requirements, high processing costs, and the generation of harmful byproducts. By comparison, the adsorption of NH_3 over porous materials is one of the most simple and efficient methods to remove the odorous gas (Zheng et al., 2016; Choi et al., 2020; Mirzaie et al., 2021), and carbon materials always draw a lot of attention owing to their high surface area, rich pores, adjustable structure and low cost (Kamran et al., 2020; Kamran and Park 2020; Kamran and Park 2021b). The physical and chemical activization of carbon materials may further increase their adsorption capacity through the enriched pore structure and active functional groups (Kamran and Park 2020; Kamran and Park 2021a; Kamran and Park 2021b; Kamran et al., 2022). In particular, acid modification of activated carbon were reported to have more hydroxyl and the acidic carboxyl groups, which significantly elevated the adsorption capacity of NH_3 (Huang et al., 2008; Kamran and Park 2021a). However, the removal ability of NH_3 by acid-modified activated carbon may decrease obviously as the operating temperature above 40°C, which severely constrains its application for purification of hot industrial gas with NH_3 (Rodrigues et al., 2007). Therefore, the deep insight into the adsorption mechanism of NH_3 over the acid-modified activated carbon will be of great significance to develop more efficient carbon materials for NH_3 removal.

The interactions between activated carbon and adsorbate are very complex owing to the various functional groups in activated carbon. Both the physical and chemical mechanisms may occur during the adsorption of NH_3 over activated carbon (Guo et al., 2005). The physical adsorption of NH_3 over the unmodified-activated carbon is so weak that the NH_3 adsorption capacity even has no obvious relationship with the surface area and pore structure (Rodrigues et al., 2007). On the other hand, the oxygen-containing functional groups (especially for the hydroxyl and carboxyl groups) on the surface of modified activated carbon may provide the main active sites for NH_3 adsorption through the chemical action (Jiang et al., 2022). The activated carbon modified by acid always exhibits excellent NH_3 adsorption capacity. Huang et al. (2008) found that the breakthrough capacity of NH_3 is linearly proportional to the amount of acidic functional groups of the acid-modified activated carbon. The further study by Qajar et al. (2015) indicates that high density of carboxylic acid groups may be produced with enhanced NH_3 adsorption capacity after modifying activated carbon by HNO_3. The hydrogen bond between the hydrogen atoms of NH_3 and oxygen atoms of the hydroxyl/carboxyl groups is regarded as the main chemical interaction during the adsorption of NH_3 over the acid-modified activated carbon (Guo et al., 2005; Tamai et al., 2006). Despite these progress on NH_3 adsorption mechanism, the previous reports ignored the influence of the residual acid on the NH_3 removal performance, and it is still unclear that how the active functional groups and residual acid functions for NH_3 removal. Moreover, the molecular level insight into the adsorption mechanism of NH_3 is still necessary to uncover the hydrogen-bond interaction between NH_3 and acid-modified activated carbon.

In this work, the modified activated carbon samples by three common inorganic acids (HNO_3, HCl and H_2SO_4) were prepared to investigate the effect of the active functional groups and residual acid on the NH_3 adsorption. The NH_3 adsorption efficiency over different modified activated carbon samples was evaluated under different conditions, and the detailed structural features of the typical activated carbon samples were investigated by SEM, BET, FT-IR, TG and NH_3-TPD. Moreover, the density functional theory (DFT) calculations were further carried out to obtain the molecular-level insight into NH_3 adsorption mechanism over the acid-modified activated carbon.

2 Experimental method

2.1 Materials and reagents

The activated carbon used in this study was purchased from Green-source Activated Carbon Company Limited, China. Prior to modification, the activated carbon was crushed and sieved into .3–.6 mm. The inorganic acids (HNO_3, HCl and H_2SO_4) and H_2O_2 were purchased from Aladdin. Deionized water was used in all the experimental processes.

2.2 Preparation of modified activated carbon

The activated carbon was modified by HNO_3, HCl, and H_2SO_4 under different conditions, respectively. Typically, 6 g of activated carbon was impregnated in 30 mL solution with different acids at the stirring speed of 200 rpm/min for 6 h. After treatment, the modified activated carbon samples were thoroughly washed by distilled water at least three times until the pH value of mother solution was close to neutral, and then dried at 100°C for 3 h. The H^+ concentration of the mother solution was kept same (10 M) when investigating the effect of acid types. Four concentrations (1 M, 5 M, 10 M and 15 M) of HNO_3 were tried, and a reflux condenser was used when the treatment temperature was 90°C. By comparison, the activated carbon samples modified by H_2O_2 were also prepared to assess the influence of surface hydroxyl groups on NH_3 removal. The modified activated carbon samples are named as "concentration-reagent-temperature" such as "5M-HNO_3-90", which means the activated carbon was modified by 5 M HNO_3 at 90°C.

2.3 Characterizations

The microstructure of activated carbon was analyzed by scanning electron microscopy (SEM, JSM-7800P, JEOL, Japan). The specific surface area, pore size and pore volume of typical activated carbon samples were measured by the automatic surface area and porosity analyzer (BET, iPore400, PhysiChem Instruments, China). The fourier transform spectroscopy (FTIR, Nicolet iS50, Thermoscientific, America) was used to characterize the surface functional groups of samples. The weight loss analysis was achieved by thermogravimetric analyzer (TG, HCT-1, BHEE, China). Temperature programmed desorption of NH_3 was performed on a chemisorption analyzer (NH_3-TPD, Autochem1 II 2920, micromeritics, America).

2.4 Adsorption performance tests

Adsorption performance of NH_3 over modified activated carbon was tested in a fixed-bed quartz reactor with 1,000 ppm NH_3 with N_2 balance. The total flow of the experiment was maintained at 200 mL/min. The adsorption temperature was controlled by a temperature controller, and the outlet concentrations of NH_3 and NO_x were continuously monitored using a Gasmet portable FTIR analyzer (Gasmet DX4000, Finland). The removal efficiency of NH_3 was determined by inlet and outlet concentration of NH_3.

$$NH_3\ \text{removal efficiency} = \frac{[NH_3]_{in} - [NH_3]_{out}}{[NH_3]_{in}} \times 100\%$$

2.5 Theoretical calculation models and methods

The models of NH_3 and HNO_3 are shown in Figures 1A, B, respectively. The original activated carbon model is derived from the graphite model (Hassel and Mark 1924). A periodic four-layer graphene structural model (5 × 5 × 4) was constructed to represent the activated carbon with different functional groups (Figures 1C–E and Supplementary Figure S1). The defected carbon was modeled by removing one of the surface central carbon atoms (Figure 1C). The carbonyl or carboxyl modified carbon models were directly built on the defected sites (Figures 1D–E). The Dmol^3 was used to optimize configuration models and find optimal adsorption configurations

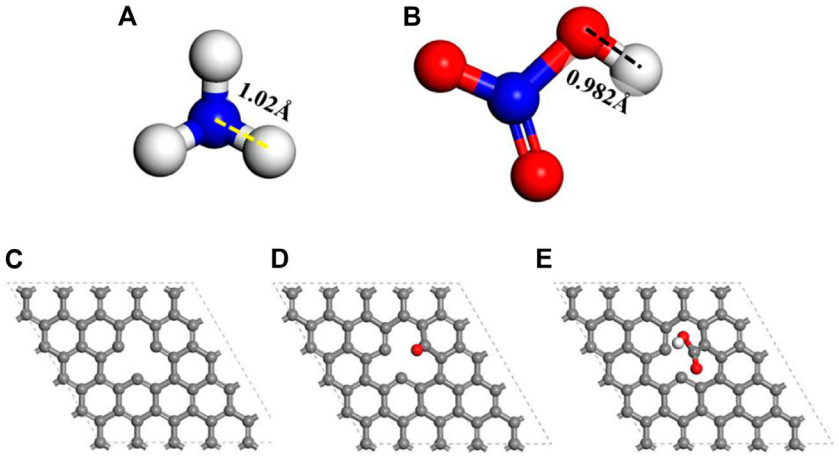

FIGURE 1
Geometrically optimized configurations of NH_3 **(A)**, HNO_3 **(B)**, defected carbon **(C)**, defected carbon with carbonyl **(D)** and defected carbon with carboxyl **(E)** from the top view. (Only the top layer is displayed. Atomic legend: -C, -H, -O, -N).

through DFT. The Perdew-Burke-Ernzerhof (PBE) in generalized gradient approximation (GGA) was used as the exchange-correlation functional (Payne et al., 1992; Perdew et al., 1996). The Tkatchenko Scheffler method was used for the DFT dispersion correction to deal with the hydrogen bond and van der Waals interactions (Tkatchenko and Scheffler 2009). The core treatment of all electron was selected with the basis set of DNP 4.4 (Li et al., 2020). The calculation parameters are with the energy tolerance of 1×10^{-5} Ha per atom, a maximum force tolerance of .002 Ha/Å, and a maximum displacement tolerance of .005 Å. A smearing of .005 Ha and the global orbital cutoff of 5.2 Å were used. Before geometry optimization, a periodic cube cell with the side length of 20 Å was built. The adsorption energy (E_{ad}) is defined as Eq. 1. $E_{adsorbate/carbon}$ is the total energy of the adsorbate/carbon system after the gas molecule being adsorbed on model carbon. $E_{adsorbate}$ is the energy of gas molecule and E_{carbon} is the energy of the model carbon after geometry optimization.

$$E_{ad} = E_{adsorbate/carbon} - E_{adsorbate} - E_{carbon} \quad (1)$$

3 Result and analysis

3.1 Adsorption performance of NH_3 over modified activated carbon

The removal performance of NH_3 over modified activated carbon samples under different conditions is shown in Figure 2. Compared with the fresh activated carbon, all the acid-modified activated carbon samples show significantly improved NH_3 adsorption capacity. Specially, the HNO_3-modified activated carbon samples have the best NH_3 adsorption capacity (Figure 2A). Huang et al. (2008) also reported that the active carbon modified by HNO_3 had much better NH_3 removal performance than that modified by other acids, which is the same with our results. Both the increased acid concentration and modification temperature are beneficial to the NH_3 adsorption over the HNO_3-modified activated carbon. But the high concentration of HNO_3 (15 M) can not further increase the NH_3 adsorption, and the best NH_3 removal performance can be achieved over the 10M-HNO_3-90 sample, whose adsorption capacity can reach 40 mg/g at room temperature. Compared with the previous reports about NH_3 adsorption over different carbon materials (Table 1), the NH_3 adsorption capacity of 10M-HNO_3-90 sample is in relatively high level. Moreover, the increased application temperature can significantly decrease the NH_3 removal performance, and the adsorption capacity can decrease to 15 mg/g over the 10M-HNO_3-90 sample at 100°C. By contrast, H_2O_2-modified activated carbon samples show only a little increase of NH_3 adsorption capacity even if treated at 90°C (Figures 2A, C). According to the previous reports (Takaoka et al., 2007; Ye et al., 2022), H_2O_2-modified activated carbon possesses mainly hydroxyl groups, and HNO_3-modified activated carbon may have much more carboxyl groups. The indistinctively increased NH_3 adsorption capacity of H_2O_2-modified activated carbon indicates that hydroxyl groups are not the active sites for NH_3 adsorption. HNO_3-modified activated carbon possess abundant carboxyl functional groups owing to the oxidation of carbon by HNO_3, and these acidic carboxyl groups may play a key role in the NH_3 adsorption (Huang et al., 2008). In addition, the dramatically weakened adsorption of NH_3 at elevated temperature implies the weak interaction between the adsorbed NH_3 and active oxygen-containing functional groups in acid-modified activated carbon.

3.2 Regeneration performance of HNO_3-modified activated carbon

The removal performance of NH_3 over the used HNO_3-modified activated carbon regenerated at different temperatures is shown in Figure 3A. After the thermal regeneration of the used HNO_3-modified activated carbon, the adsorption capacity of NH_3 dramatically

10.3389/fenvs.2023.976113

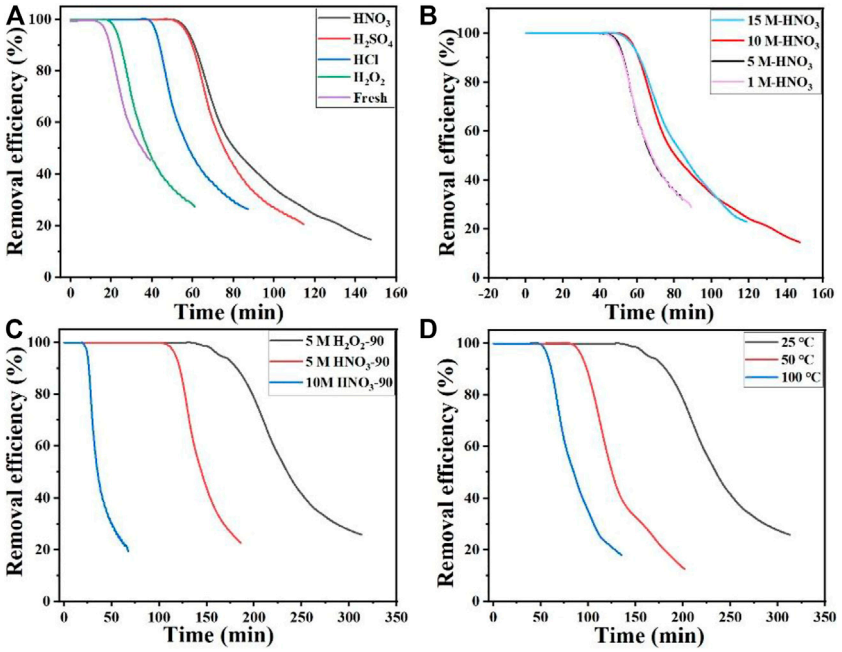

FIGURE 2
Removal efficiency of NH_3 over modified activated carbon samples under different conditions: **(A)** modification by different acids, **(B)** modification by HNO_3 of different concentrations, **(C)** modification at 90°C, and **(D)** the removal of NH_3 over 10M-HNO_3-90 at different temperatures.

TABLE 1 The NH_3 adsorption capacity over different carbon materials in the literatures.

Samples	Measurement type	Temperatures	NH_3 adsorption capacity (mg/g)	References
Coconut shell carbon	Breakthrough	40°C	1.8	Rodrigues et al. (2007)
HNO_3-carbon	Breakthrough	30°C	41.6	Huang et al. (2008)
Carbon molecular sieve	Breakthrough	25°C	12.9	Khabzina and Farrusseng (2018)
Graphite oxide	Breakthrough	25°C	60.8	Petit and Bandosz (2009)
STAM-17-OEt/carbon	Breakthrough	25°C	17.6	McHugh et al. (2019)
Al-Zr/carbon	Breakthrough	25°C	19.7	Petit and Bandosz (2008)

decreases compared with its corresponding fresh one (results in Figure 2A). And the NH_3 adsorption capacity of sample regenerated at 200°C is almost the same with the fresh activated carbon. Moreover, the abundant NO_x (mainly NO and NO_2) as well as NH_3 were detected during the thermal regeneration process of the used HNO_3-modified activated carbon (Figure 3B). According to the previous reports, HNO_3-modified activated carbon possess abundant hydroxyl and carboxyl groups (Guo et al., 2015; Demiral et al., 2021). The NH_3 removal performance over H_2O_2-modified activated carbon (Figure 2) implies the hydroxyl groups may have little influence on the NH_3 removal capacity. Thus, the acidic carboxyl groups can be the main active sites for NH_3 adsorption over the HNO_3-modified activated carbon. On the other hand, the release of NO_x verifys the that HNO_3 molecule was left on the HNO_3-modified activated carbon even after thorough washing. Considering the strong acidity of HNO_3, the residual HNO_3 on the modified activated carbon may also dramatically affect the adsorption capacity of NH_3, which was always ignored by previous reports.

3.3 Structural characteristics of the modified activated carbon

The morphology of the modified activated carbon samples was observed by the SEM as shown in Figure 4. The surface of the fresh activated carbon is smooth (Figure 4A). The modification of activated carbon by H_2O_2 does not obviously change its morphology (Figure 4B). But the surface of the activated carbon modified by HNO_3 becomes very rough, especially for the sample of 10M-HNO_3-90 (Figures 4C, D). HNO_3 possesses the strong oxidizing/etching properties, and its oxidizing/etching capacity will be enhanced at elevated temperature (Vinke et al., 1994; Zhang et al., 2008). Thus, the treatment of activated carbon by HNO_3 at 90°C will oxidize partial surface carbon atoms and etch some mineral substance in activated carbon, which results in the rough surface of HNO_3-modified activated carbon.

To have deep insight into the change of surface area and pore structure after modification, the BET tests were performed, and the

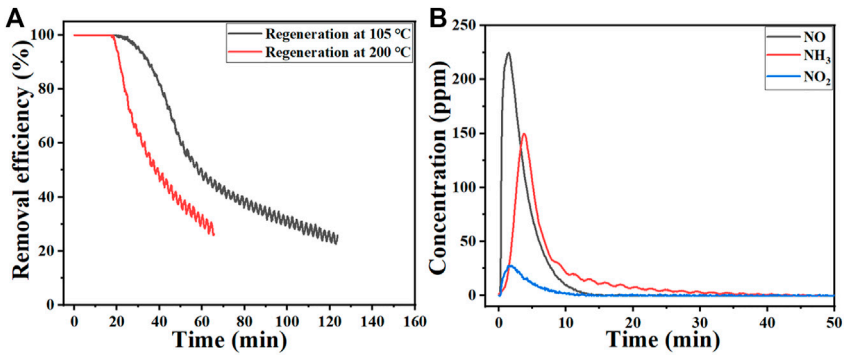

FIGURE 3
Removal efficiency of NH_3 over the used HNO_3-modified activated carbon regenerated at different temperatures **(A)** and the gas products released during the thermal regeneration process **(B)**.

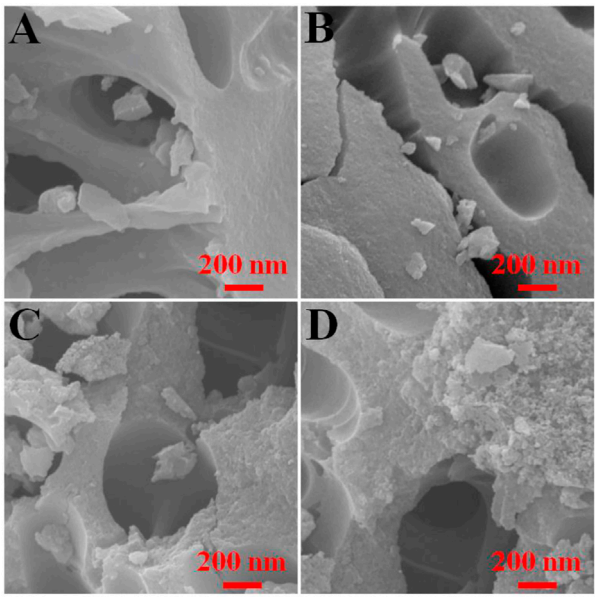

FIGURE 4
Morphology features of the typical activated carbon samples: **(A)** Fresh, **(B)** 5M-H_2O_2-90, **(C)** 10M-HNO_3-25, **(D)** 10M-HNO_3-90.

surface area and pore features of the typical activated carbon are shown in Figure 5 and Table 2. As it can be seen, these carbon samples exhibit the typical IV isotherms with the H3 hysteresis loops (Figure 5A), and more pores are produced after modification by H_2O_2 or HNO_3 (Figure 5B). It can been seen from Table 2 that the modified activated carbon samples by both H_2O_2 and HNO_3 can increase the specific surface, pore volume and pore size. The modified activated carbon by HNO_3 at 90°C exhibits the largest specific surface (581.27 m^2/g), pore volume (.34 cm^3/g) and pore size (2.10 nm). According to a previous reports, the oxidation reaction will occur between HNO_3 and activated carbon during the acid-modification process, which can enlarge the original pores or form new pore structure (Wang et al., 2017b; Giraldo et al., 2020). The BET results are also in accordance with the SEM observation, further implying that the oxidation and corrosion of activated carbon by HNO_3 enrich the pore structure of activated carbon.

Surface functional groups on the modified activated carbon samples were also detected by FTIR, and the spectra are shown in Figure 6. The signal at 1,570 cm^{-1} is the C=C stretch, and the signal at about 1725 cm^{-1} is the stretching of carboxyl (Laszlo et al., 2004; Guo et al., 2005). The infrared signal at about 1,240 cm^{-1} can be assigned to the stretching of saturated oxygen-containing functional groups such as ethers (Moreno-Castilla et al., 1998). Bands in the 900–1,200 cm^{-1} region are difficult to assign because there is a superposition of a number of broad overlapping bands, which thus cannot be described in terms of simple motion of specific functional groups or chemical bonds (Moreno-Castilla et al., 1998). Compared with the fresh activated carbon, the oxidation of active carbon by both H_2O_2 and HNO_3 can increase the amount of oxygen-containing functional groups. But the oxidation of activated carbon by HNO_3 can produce more oxygen-containing functional groups than H_2O_2, especially for carboxyl groups. Considering the observation of abundant NO_x (mainly NO and NO_2) during the thermal regeneration of the used HNO_3-modified activated carbon (Figure 3B), the contribution of the strong signal intensity of oxygen-containing functional groups may also result from the residual HNO_3 molecule adsorbed on activated carbon. For the used 10M-HNO_3-90 sample, a new shoulder peak appears at 1,273 cm^{-1}, which may be some kind of adsorbed NH_3 complex. It is generally recognized that hydroxyl and carboxyl groups in activated carbon provide the main active sites for NH_3 adsorption through the chemical action (Jiang et al., 2022). Although the H_2O_2-modified activated carbon may possesses much more hydroxyl groups (Wang et al., 2012; Liu et al., 2018), its weak NH_3 adsorption capacity implys the hydroxyl groups in activated carbon are not so acitve for NH_3 adsorption. Only the acidic oxygen-containing groups such as carboxyl and adsorbed HNO_3 may play a dominant role in its enhanced NH_3 adsorption capacity. After the NH_3 molecule diffuses into the pore of AC, the adsorbed NH_3 may strongly interact with the neighbor acidic groups (carboxyl and adsorbed HNO_3) with increased NH_3 adsorption capacity.

For the TG curves of the typical activated carbon samples (Figure 7), the weight loss of all the samples occurs within 200°C, implying the easy elimination of these acquired functional groups including carboxyl and residual HNO_3 after modification (Doğan

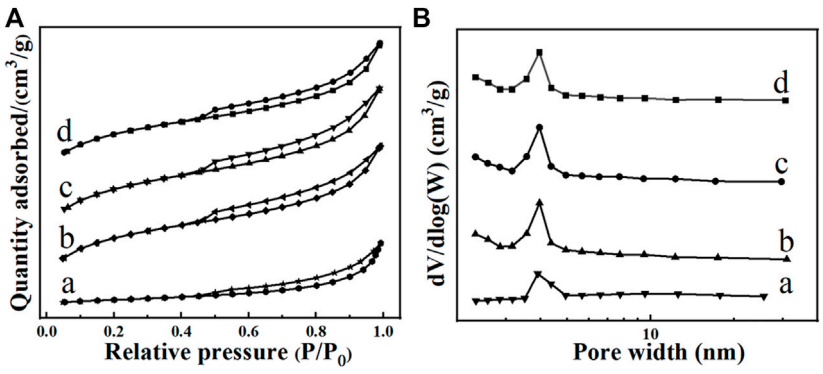

FIGURE 5
N_2 adsorption-desorption isotherms **(A)** and corresponding pore size distributions **(B)** of the typical activated carbon samples: (A) Fresh, (B) 5M-H_2O_2-90, (C) 10M-HNO_3-25, (D) 10M-HNO_3-90.

TABLE 2 Surface area and pore features of the typical activated carbon samples.

Samples	S_{BET}	Pore volume	Pore size
	(m^2/g)	cm^3/g	Nm
Fresh	525.20	.27	1.84
5M-H_2O_2-90	528.41	.26	1.85
10M-HNO_3-25	559.32	.31	1.91
10M-HNO_3-90	581.27	.34	2.10

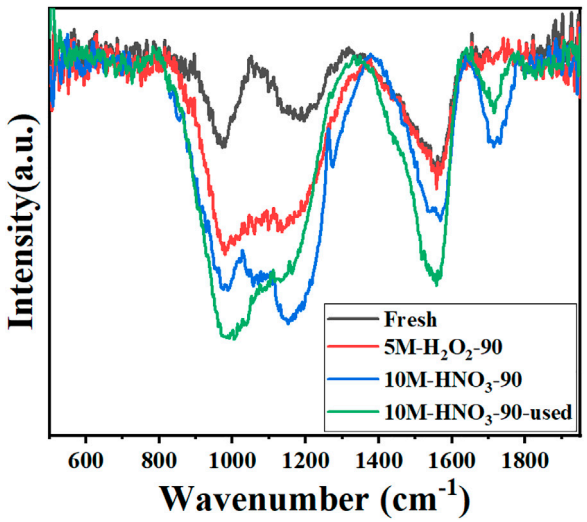

FIGURE 6
FTIR results of the typical activated carbon samples.

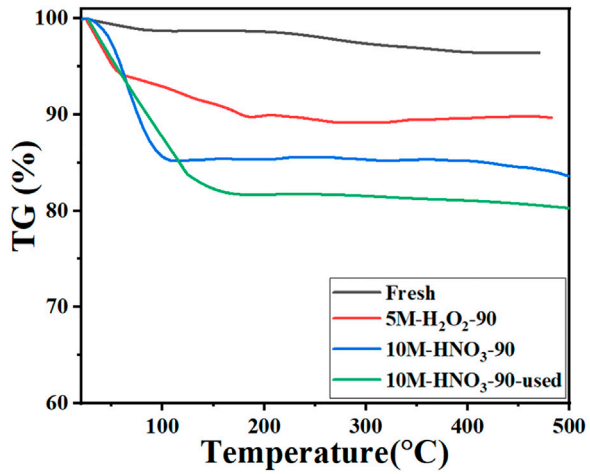

FIGURE 7
TG results of the typical activated carbon samples.

et al., 2020). The more weight loss for 10M-HNO_3-90 than 5M-H_2O_2-90 indicates the more oxygen-containing functional groups in the sample of 10M-HNO_3-90, which is consistent with the FTIR results in Figure 6. For the used 10M-HNO_3-90 sample, much more weight loss about 4 wt% can be observed than its corresponding fresh 10M-HNO_3-90 sample. The result is also well coincidence with the calculated adsorption capacity of 40 mg/g according to the NH_3 removal performance in Figure 2A. Moreover, the easy elimination of the active functional groups in activated carbon even at low thermal-treatment temperature below 200°C accounts for the bad regeneration performance of the acid-modified activated carbon as shown in Figure 3A.

To further make clear the NH_3 adsorption mechanism, the NH_3-TPD tests were carried out for the typical activated carbon samples as shown in Figure 8. Similar with the TG results in Figure 7, most NH_3 adsorbed on all the three samples can be easily desorbed below 200°C, which indicates the weak binding force between NH_3 and active functional groups in activated carbon. The amount of the adsorbed NH_3 over both the fresh and H_2O_2-modified activated carbon is far below that over the 10M-HNO_3-90 sample. Ye et al. (2022) also reported the weak NH_3 adsorption on the activated carbon modified by different acids, which is nearly the same with Figure 8. These results demonstrate the modification of activated carbon by HNO_3 can significantly increase the number of active sites for NH_3

10.3389/fenvs.2023.976113

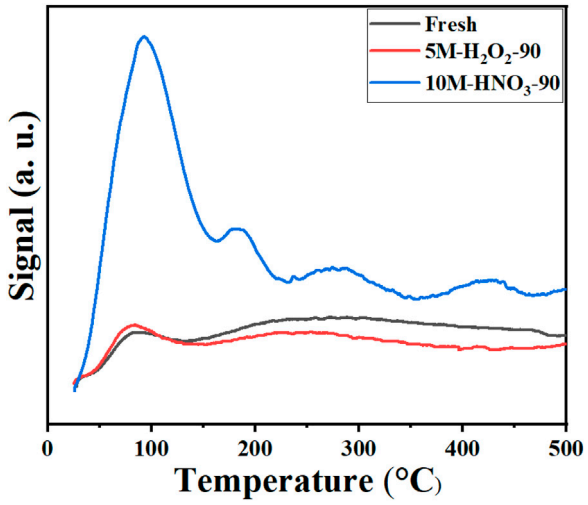

FIGURE 8
NH_3-TPD profiles of the typical activated carbon samples.

adsorption, but cannot increase the binding force between NH_3 and active functional groups in activated carbon.

3.4 Theoretical insight into the NH_3 adsorption over the acid-modified activated carbon

According to the above performance and structure data, the oxidation of activated carbon by HNO_3 will produce more oxygen-containing functional groups including carboxyl and residual HNO_3, and these acid sites may strongly interact with NH_3 and facilitate its adsorption. Thus, the activated carbon models with defected, carbonyl and carboxyl groups were established to investigate the detailed adsorption mechanism of NH_3 on the activated carbon with different functional groups (See the structural models in Figure 1 and Supplementary Figure S1).

Compared with the activated carbon with defect or carbonyl groups, the acidic carboxyl group indeed has strong binding force with NH_3 with the lowest adsorption energy (−.66 eV) and the shortest N···H hydrogen bond length (1.66 Å) (Figures 9A1–A3). For the adsorption of the residual HNO_3, the binding force between the carboxyl functional group and HNO_3 molecule are also the strongest with the lowest adsorption energy (−.79 eV) (Figures 9B1–B3). A circular hydrogen-bond network is formed between HNO_3 and carboxyl group, in which the O···H hydrogen bond lengths are 1.98 Å and 1.58 Å, respectively (Figure 9B3). For the co-adsorption of NH_3 and HNO_3, the adsorption energies over all the three carbon models obviously decrease, and the co-adsorption energy of NH_3 and HNO_3 over activated carbon with carboxyl group is also the lowest (−1.63 eV) (Figures 9C1–C3). In particular, H atom in HNO_3 is dissociated to form NH_4^+ ions, and a large circular hydrogen-bond network among NO_3^-, NH_4^+ and carbonyl in activated carbon is formed. The hydrogen bond lengths of the three O···H bonds in the network are 1.53 Å, 1.58 Å and 1.67 Å, respectively, whose average value is the lowest of all (Figure 9C3). As is well-known, the lower adsorption energy and the shorter length of hydrogen bond mean the stronger adsorption with bigger binding force (Pan and Xing 2008). The carboxyl in carbon can strong interact with both NH_3 and HNO_3 through the hydrogen bond, and the formation of the circular hydrogen-bond network among NO_3^-, NH_4^+ and carbonyl further decreases the adsorption energy with enhanced adsorption capacity of NH_3.

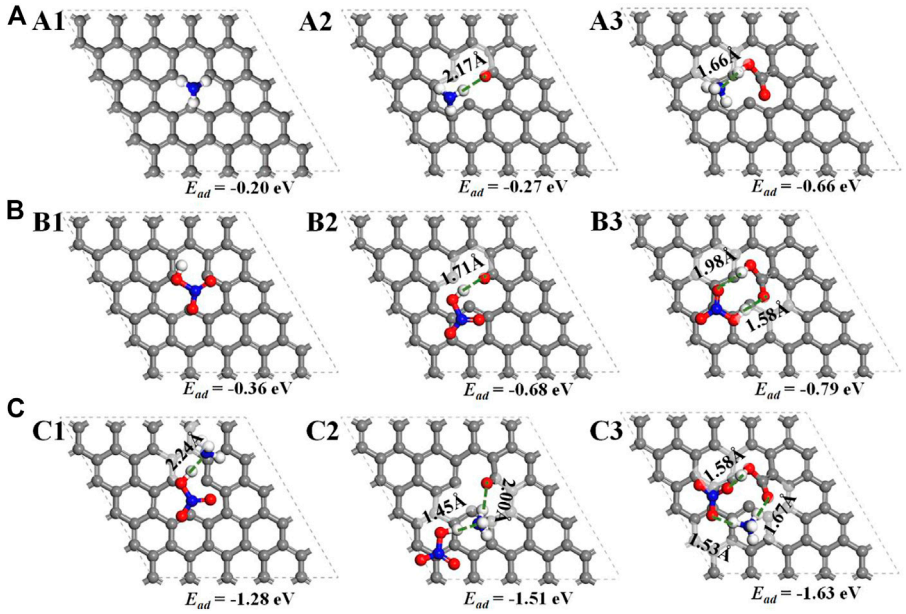

FIGURE 9
Geometrically optimized configurations of adsorbed NH_3 **(A1–A3)**, adsorbed HNO_3 **(B1–B3)** and co-adsorbed NH_3/HNO_3 **(C1–C3)** on defected carbon, defected carbon with carbonyl and defected carbon with carboxyl from the top view with their adsorption energy and hydrogen-bond length labeled, respectively. (Only the top layer is displayed. Atomic legend: -C, -H, -O, -N).

Taking all the perforemance, structure and calculation results together, the oxidation reaction occurs between HNO_3 and activated carbon during the acid-modification process, and more pores and active surface carboxyl groups are formed in HNO_3-modified activated carbon. The thermal treatment of the used HNO_3-modified activated carbon confirms the existence of the residual HNO_3 in modified activated carbon. The acidic carboxyl groups and residual HNO_3 play a dominant role in its enhanced NH_3 adsorption capacity. On the other hand, these acidic species in activated carbon can be easily eliminated even at low thermal-treatment temperature below 200°C, which accounts for its bad regeneration performance of the acid-modified activated carbon. DFT calculations further display that the carboxyl functional group can strongly interplay with NH_3 or HNO_3 with the lowest adsorption energy (−.66 eV and −.79 eV, respectively), and the co-adsorption of NH_3 and HNO_3 around the carboxyl functional group forms a strong circular hydrogen-bond network among NO_3^-, NH_4^+ and carbonyl and further decreases the adsorption energy (−1.63 eV), which provides a molecular level insight into the adsorption mechanism of NH_3 over the acid-modified activated carbon.

4 Conclusion

In summary, the effect of the active functional groups and residual acid on the NH_3 adsorption over the acid-modified activated carbon was investigated to make clear its enhanced NH_3 adsorption mechanism by both experimental and theoretical methods. The activated carbon modified by HNO_3 possesses the best NH_3 removal performance with the maximum NH_3 adsorption amounts of 40 mg/g over the 10M-HNO_3-90 sample. The multiple structural characterizations (SEM, BET, FTIR, TG, NH_3-TPD) of the typical activated carbon samples further reveal that the activated carbon can be oxidized and etched by HNO_3 with enriched pore structure, carbonyl groups and residual HNO_3. These acidic species including carbonyl and residual HNO_3 play a key role in the improved NH_3 adsorption capacity. DFT calculations further reveal the carboxyl functional group can strongly interplay with both NH_3 and HNO_3 with the lowest adsorption energies (−.66 eV and −.79 eV, respectively), and the co-adsorption of NH_3 and HNO_3 on the carboxyl functional group forms a strong circular hydrogen-bond network among NO_3^-, NH_4^+ and carbonyl and further decreases the adsorption energy (−1.63 eV). The experimental and theoretical results together demonstrate that the oxidation and etching of activated carbon by acid enrich the active surface carboxyl functional groups, and the co-adsorption of NH_3 with the residual HNO_3 around the carboxyl functional group through the strong circular hydrogen-bond network accounts for the enhanced NH_3 adsorption capacity of the acid-modified activated carbon. The demonstrated adsorption behaviours and mechanism suggests that the modified activated carbon with more acidic oxygen-containing functional groups will significantly elevate the NH_3 adsorption capacity for its further commercial applications.

Data availability statement

The original contributions presented in the study are included in the article/Supplementary Material, further inquiries can be directed to the corresponding authors.

Author contributions

Academic idea, DFT calculation, and original draft preparation by CL; Sample preparation, characterizations and performance tests by SZ, ML, and YL; Calculation methods by S-MX; Suggestions by CZ and JL; Funding, modification and supervision by ZY and JY. All authors read and approved the final manuscript.

Funding

This work was supported by Natural Science Foundation of Beijing Municipality (No. 8222042), Zhongye Changtian Basic Research Foundation (No. 2021JCYJ10) and National Natural Science Foundation of China (No. 21601192).

Conflict of interest

CZ was employed by Everbright Environmental Technology Co., Ltd. JL was employed by Zhongye Changtian International Engineering Co., Ltd.

The remaining authors declare that the research was conducted in the absence of any commercial or financial relationships that could be construed as a potential conflict of interest.

Publisher's note

All claims expressed in this article are solely those of the authors and do not necessarily represent those of their affiliated organizations, or those of the publisher, the editors and the reviewers. Any product that may be evaluated in this article, or claim that may be made by its manufacturer, is not guaranteed or endorsed by the publisher.

Supplementary material

The Supplementary Material for this article can be found online at: https://www.frontiersin.org/articles/10.3389/fenvs.2023.976113/full#supplementary-material

References

Choi, J. H., Jang, J. T., Yun, S. H., Jo, W. H., Lim, S. S., Park, J. H., et al. (2020). Efficient removal of ammonia by hierarchically porous carbons from a CO_2 capture process. *Chem. Eng. Technol.* 43, 2031–2040. doi:10.1002/ceat.202000104

Dai, C., Huang, S., Zhou, Y., Xu, B., Peng, H., Qin, P., et al. (2019). Concentrations and emissions of particulate matter and ammonia from extensive livestock farm in south China. *Environ. Sci. Pollut. Res.* 26, 1871–1879. doi:10.1007/s11356-018-3766-4

Demiral, I., Samdan, C., and Demiral, H. (2021). Enrichment of the surface functional groups of activated carbon by modification method. *Surf. Interfaces* 22, 100873. doi:10.1016/j.surfin.2020.100873

Doğan, M., Sabaz, P., Bïcïl, Z., Koçer Kizilduman, B., and Turhan, Y. (2020). Activated carbon synthesis from tangerine peel and its use in hydrogen storage. *J. Energy Inst.* 93, 2176–2185. doi:10.1016/j.joei.2020.05.011

Giannakis, E., Kushta, J., Bruggeman, A., and Lelieveld, J. (2019). Costs and benefits of agricultural ammonia emission abatement options for compliance with European air quality regulations. *Environ. Sci. Eur.* 31, 93. doi:10.1186/s12302-019-0275-0

Giraldo, L., Vargas, D. P., Moreno-Pirajan, J. C., Mancin, F., and Madder, A. (2020). Study of CO_2 adsorption on chemically modified activated carbon with nitric acid and ammonium aqueous. *Front. Chem.* 8, 4. doi:10.3389/fchem.2020.00004

Guo, J., Xu, W. S., Chen, Y. L., and Lua, A. C. (2005). Adsorption of NH_3 onto activated carbon prepared from palm shells impregnated with H_2SO_4. *J. Colloid Interface Sci.* 281, 285–290. doi:10.1016/j.jcis.2004.08.101

Guo, Q., Jing, W., Hou, Y., Huang, Z., Ma, G., Han, X., et al. (2015). On the nature of oxygen groups for NH_3-SCR of NO over carbon at low temperatures. *Chem. Eng. J.* 270, 41–49. doi:10.1016/j.cej.2015.01.086

Han, B., Butterly, C., Zhang, W., He, J.-Z., and Chen, D. (2021). Adsorbent materials for ammonium and ammonia removal: A review. *J. Clean. Prod.* 283, 124611. doi:10.1016/j.jclepro.2020.124611

Hassel, O., and Mark, H. (1924). Über die kristallstruktur des graphits. *Z. für Phys.* 25, 317–337. doi:10.1007/bf01327534

Huang, C.-C., Li, H.-S., and Chen, C.-H. (2008). Effect of surface acidic oxides of activated carbon on adsorption of ammonia. *J. Hazard. Mat.* 159, 523–527. doi:10.1016/j.jhazmat.2008.02.051

Jiang, Q., Li, T., He, Y., Wu, Y., Zhang, J., and Jiang, M. (2022). Simultaneous removal of hydrogen sulfide and ammonia in the gas phase: A review. *Environ. Chem. Lett.* 20, 1403–1419. doi:10.1007/s10311-021-01366-w

Kamran, U., Choi, J. R., and Park, S.-J. (2020). A role of activators for efficient CO(2) affinity on polyacrylonitrile-based porous carbon materials. *Front. Chem.* 8, 710. doi:10.3389/fchem.2020.00710

Kamran, U., Rhee, K. Y., Lee, S.-Y., and Park, S.-J. (2022). Solvent-free conversion of cucumber peels to n-doped microporous carbons for efficient CO_2 capture performance. *J. Clean. Prod.* 369, 133367. doi:10.1016/j.jclepro.2022.133367

Kamran, U., and Park, S.-J. (2020). Tuning ratios of KOH and NaOH on acetic acid-mediated chitosan-based porous carbons for improving their textural features and CO_2 uptakes. *J. CO2 Util.* 40, 101212. doi:10.1016/j.jcou.2020.101212

Kamran, U., and Park, S.-J. (2021a). Acetic acid-mediated cellulose-based carbons: Influence of activation conditions on textural features and carbon dioxide uptakes. *J. Colloid Interface Sci.* 594, 745–758. doi:10.1016/j.jcis.2021.03.069

Kamran, U., and Park, S.-J. (2021b). Chemically modified carbonaceous adsorbents for enhanced CO_2 capture: A review. *J. Clean. Prod.* 290, 125776. doi:10.1016/j.jclepro.2020.125776

Khabzina, Y., and Farrusseng, D. (2018). Unravelling ammonia adsorption mechanisms of adsorbents in humid conditions. *Microporous Mesoporous Mater* 265, 143–148. doi:10.1016/j.micromeso.2018.02.011

Laszlo, K., Marthi, K., Rochas, C., Ehrburger-Dolle, F., Livet, F., and Geissler, E. (2004). Morphological investigation of chemically treated poly(ethylene terephthalate)-based activated carbons. *Langmuir* 20, 1321–1328. doi:10.1021/la035954s

Li, K., Li, N., Yan, N., Wang, T., Zhang, Y., Song, Q., et al. (2020). Adsorption of small hydrocarbons on pristine, n-doped and vacancy graphene by DFT study. *Appl. Surf. Sci.* 515, 146028. doi:10.1016/j.apsusc.2020.146028

Liang, S., Li, R., Xia, B., Guo, M., Cheng, F., and Zhang, M. (2020). Dynamic desulfurization process over porous Zn-Cu-based materials in a packed column: Adsorption kinetics and breakthrough modeling. *Energy fuels.* 34, 16552–16559. doi:10.1021/acs.energyfuels.0c03197

Liu, Z., Zhang, Y.-G., Han, B., Tan, Z.-C., and Li, Q.-H. (2018). Adsorption of cobalt (III) by HCl and H_2O_2 modified activated carbon. *Int. J. Environ. Pollut.* 63, 192–205. doi:10.1504/ijep.2018.10018461

McHugh, L. N., Terracina, A., Wheatley, P. S., Buscarino, G., Smith, M. W., and Morris, R. E. (2019). Metal-organic framework-activated carbon composite materials for the removal of ammonia from contaminated airstreams. *Angew. Chem. Int. Ed.* 58, 11873–11877. doi:10.1002/ange.201905779

Mirzaie, M., Talebizadeh, A. R., and Hashemipour, H. (2021). Mathematical modeling and experimental study of VOC adsorption by pistachio shell-based activated carbon. *Environ. Sci. Pollut. Res.* 28, 3737–3747. doi:10.1007/s11356-020-10634-1

Moreno-Castilla, C., Carrasco-Marin, F., Maldonado-Hodar, F. J., and Rivera-Utrilla, J. (1998). Effects of non-oxidant and oxidant acid treatments on the surface properties of an activated carbon with very low ash content. *Carbon* 36, 145–151. doi:10.1016/s0008-6223(97)00171-1

Pan, B., and Xing, B. (2008). Adsorption mechanisms of organic chemicals on carbon nanotubes. *Environ. Sci. Technol.* 42, 9005–9013. doi:10.1021/es801777n

Payne, M. C., Teter, M. P., Allan, D. C., Arias, T. A., and Joannopoulos, J. D. (1992). Iterative minimization techniques for *ab initio* total-energy calculations: Molecular dynamics and conjugate gradients. *Rev. Mod. Phys.* 64, 1045–1097. doi:10.1103/revmodphys.64.1045

Perdew, J. P., Burke, K., and Ernzerhof, M. (1996). Generalized gradient approximation made simple. *Phys. Rev. Lett.* 77, 3865–3868. doi:10.1103/physrevlett.77.3865

Petit, C., and Bandosz, T. J. (2008). Activated carbons modified with aluminium-zirconium polycations as adsorbents for ammonia. *Microporous Mesoporous Mater* 114, 137–147. doi:10.1016/j.micromeso.2007.12.029

Petit, C., and Bandosz, T. J. (2009). Graphite oxide/polyoxometalate nanocomposites as adsorbents of ammonia. *J. Phys. Chem. C* 113, 3800–3809. doi:10.1021/jp8097044

Qajar, A., Peer, M., Andalibi, M. R., Rajagopalan, R., and Foley, H. C. (2015). Enhanced ammonia adsorption on functionalized nanoporous carbons. *Microporous Mesoporous Mater* 218, 15–23. doi:10.1016/j.micromeso.2015.06.030

Rodrigues, C. C., de Moraes, D., Jr., da Nobrega, S. W., and Barboza, M. G. (2007). Ammonia adsorption in a fixed bed of activated carbon. *Bioresour. Technol.* 98, 886–891. doi:10.1016/j.biortech.2006.03.024

Stokstad, E. (2014). Ammonia pollution from farming may exact hefty health costs. *Science* 343, 238. doi:10.1126/science.343.6168.238

Takaoka, M., Yokokawa, H., and Takeda, N. (2007). The effect of treatment of activated carbon by H_2O_2 or HNO_3 on the decomposition of pentachlorobenzene. *Appl. Catal. B* 74, 179–186. doi:10.1016/j.apcatb.2007.02.009

Tamai, H., Nagoya, H., and Shiono, T. (2006). Adsorption of methyl mercaptan on surface modified activated carbon. *J. Colloid Interface Sci.* 300, 814–817. doi:10.1016/j.jcis.2006.04.056

Tkatchenko, A., and Scheffler, M. (2009). Accurate molecular van der Waals interactions from ground-state electron density and free-atom reference data. *Phys. Rev. Lett.* 102, 073005. doi:10.1103/physrevlett.102.073005

Vikrant, K., Kumar, V., Kim, K.-H., and Kukkar, D. (2017). Metal-organic frameworks (MOFs): Potential and challenges for capture and abatement of ammonia. *J. Mat. Chem. A* 5, 22877–22896. doi:10.1039/c7ta07847a

Vinke, P., Vandereijk, M., Verbree, M., Voskamp, A. F., and Vanbekkum, H. (1994). Modification of the surfaces of a gas-activated carbon and a chemically activated carbon with nitric-acid, hypochlorite, and ammonia. *Carbon* 32, 675–686. doi:10.1016/0008-6223(94)90089-2

Wang, G., Wu, T., Li, Y., Sun, D., Wang, Y., Huang, X., et al. (2012). Removal of ampicillin sodium in solution using activated carbon adsorption integrated with H_2O_2 oxidation. *J. Chem. Technol. Biotechnol.* 87, 623–628. doi:10.1002/jctb.2754

Wang, J., Jiang, W., Zhang, Z., and Long, D. (2017a). Mesoporous carbon beads impregnated with transition metal chlorides for regenerative removal of ammonia in the atmosphere. *Ind. Eng. Chem. Res.* 56, 3283–3290. doi:10.1021/acs.iecr.7b00013

Wang, X., Yao, R., Bai, Z., and Ma, H. (2017b). The active sites and mechanism of NO oxidation on modified activated carbon. *React. Kinet. Mech. Cat.* 120, 209–217. doi:10.1007/s11144-016-1091-9

Ye, Y., Xie, J., De, F., Wang, X., He, F., and Jin, Q. (2022). Effect of acid treatment on surfaces of activated carbon supported catalysts for NO and SO_2 removal. *Fuller. nanotub. car. nano.* 30, 297–305. doi:10.1080/1536383x.2021.1938000

Zhang, N., Wang, L.-y., Liu, H., and Cai, Q.-K. (2008). Nitric acid oxidation on carbon dispersion and suspension stability. *Surf. Interface Anal.* 40, 1190–1194. doi:10.1002/sia.2864

Zheng, W., Hu, J., Rappeport, S., Zheng, Z., Wang, Z., Han, Z., et al. (2016). Activated carbon fiber composites for gas phase ammonia adsorption. *Microporous Mesoporous Mater* 234, 146–154. doi:10.1016/j.micromeso.2016.07.011

Zhong, F.-Y., Peng, H.-L., Tao, D.-J., Wu, P.-K., Fan, J.-P., and Huang, K. (2019). Phenol-based ternary deep eutectic solvents for highly efficient and reversible absorption of NH_3. *ACS Sustain. Chem. Eng.* 7, 3258–3266. doi:10.1021/acssuschemeng.8b05221